

Cleaning Multi-channel Heliophysical Data with Pixel-wise Autoencoder

MICHAEL S. PENWARDEN¹ AND MARK C. M. CHEUNG¹

¹ Lockheed Martin Solar & Astrophysics Laboratory
 3251 Hanover Street, Palo Alto
 CA 94304, USA

Submitted to AJ

ABSTRACT

We present a new method of removing shot noise from SDO/AIA images using a pixel-wise autoencoder architecture. Shot noise is present in all imaging and the proportion of noise to signal increases over the lifetime of a mission, this makes the problem worse for recent data. By using pixels across multiple wavelengths, we hope to retain the ground truth signal while still being able to denoise. We find that the low SNR channels greatly benefit from the denoising of this model. Additionally, the method can be used on any shape or sized image. Comparing this to a convolutional architecture, which distorts the image by "smoothing" and is limited by the shape and size of the input, our proposed method has significant benefits.

Keywords: Shot noise, Autoencoder, AIA

1. INTRODUCTION

The Atmospheric Imaging Assembly (AIA) aboard the Solar Dynamics Observatory (SDO) images the solar chromosphere and corona across seven extreme ultraviolet (EUV) channels. Over the lifetime of the mission the coating on the instruments degrade causing a decrease in signal-to-noise ratio (SNR) (Boerner et al. 2014).

The images used are taken from the Helio-physics Events Knowledgebase (HEK) which contains a database of solar events. To gather the train and test datasets, HEK is used to search for ideal images. (Hurlbut et al. 2012).

(DeForest 2017)

2. PROBLEM STATEMENT

Let the level 1 AIA image in channel c be denoted as $\mathcal{I}_c(i, j)$, where (i, j) denotes the pixel location. Level 1 AIA images have been processed from the raw level 0 data by means of dark current, pedestal subtraction, flat field correction, and despiking of the cosmic-rays. (Lemen et al. 2012). Level 0 and therefore level 1 images

also contain shot noise from the measurements. Let us denote the original astronomical object image by

$$\mathcal{O}_c(i, j) = \mathcal{I}_c(i, j) - \mathcal{S}(i, j), \quad (1)$$

where \mathcal{S} denotes the Poisson distribution describing the shot noise.

In principle, one would like a model to recover $\mathcal{O}_c(i, j)$. This is difficult for a number of reasons. The solar corona changes on timescales as short as seconds, so the underlying ground truth object changes from exposure to exposure. This means one cannot recover the ground truth by simply adding multiple exposures to increase the SNR. Instead, we consider the following experiment. Suppose additional Poissonian noise were artificially added to the level 1 images $\mathcal{I}_c(i, j)$. Denote this as

$$\mathcal{A}_c(i, j) = \mathcal{I}_c(i, j) + \mathcal{P}_c(i, j). \quad (2)$$

where $\mathcal{P}_c(i, j)$ denotes the artificial noise added to pixel (i, j) by sampling from the Poissonian distribution with expectation value $\mathcal{I}_c(i, j)$.

The addition of artificial noise is a pixel-wise and channel-wise operation. We expect $\mathcal{S}_c(i, j)$ to be uncorrelated with $\mathcal{P}_c(i, j)$, i.e. $\langle \mathcal{S}_c \mathcal{P}_c \rangle = 0$. In addition, we expect $\langle \mathcal{S}_c \mathcal{S}_{c'} \rangle = \langle \mathcal{P}_c \mathcal{P}_{c'} \rangle = 0$ for c and c' denoting different wavelength channels.

In our experiments, we hope that, by using the known artificially noisy images $\mathcal{A}_c(i, j)$, and the fact that noise is uncorrelated across different wavelength channels, we can train a model which denoises sets of multi-channel images in order to approximate $\mathcal{I}_c(i, j)$. Should this be successful, one can then apply the model to more recent sets of images to recover $\mathcal{O}_c(i, j)$. In theory, the model should learn to remove the artificial Poisson noise, and when applied to recent unmodified images, instead remove the original shot noise, thus cleaning the image.

In order to denoise sets of multi-channel AIA images, the images should be spatially aligned so that the underlying signal is correlated across channels. Due to minor misalignment and varying plate scales between AIA channels, geometric transformation (including translation, scaling and rotation) must be applied to level 1 images. Furthermore, exposure time normalization should be applied. We denote this combined transformation as $\mathcal{T}(x)$. Let any transformed be denoted as

$$X'_c(i, j) = \mathcal{T}(X_c(i, j)) \quad (3)$$

Our model \mathcal{M} is trained to perform the conversion

$$\mathcal{M} : \mathcal{A}'_c(i, j) \rightarrow \mathcal{I}'_c(i, j) \quad (4)$$

A denoised image is then defined as

$$\hat{X}_c(i, j) = \mathcal{M}(X_c(i, j)) \quad (5)$$

and our final objective is to build a model in which this relation is satisfied

$$\hat{\mathcal{A}}'_c(i, j) \approx \mathcal{I}'_c(i, j) \quad (6)$$

Should this succeed, the following relation should also hold true for recent images given the artificial noise correctly emulates the shot noise.

$$\hat{\mathcal{I}}'_c(i, j) \approx \mathcal{O}'_c(i, j) \quad (7)$$

3. METHODOLOGY

3.1. Artificial Noise

To create a data set with which to train the model, artificial noise is added to early images in the missions life to emulate the noisy, more recent, images. The image pixel values are in units of "Data Numbers" (DN) which are counts of incident photons converted by a Charge-Coupled Device (CCD). For a given pixel location, the randomness in the measurement is called shot noise. This is given by the following relation

$$\text{Shot Noise} = \sqrt{\text{Signal}} \quad (8)$$

Since shot noise is proportional to the square root of the signal, as it drops over time the SNR also decreases

making the shot noise more prominent. This is especially evident in the channels which already have low SNR such as 94Å and 335Å. To simulate this noise, the artificial noise is created by drawing from a Poisson distribution for each pixel where the expectation value is the absolute value of the pixel. This noise is shown by the equation

$$\mathcal{P}_c(i, j) = \text{abs}(\mathcal{I}_c(i, j)) + \text{Poisson}(\text{abs}(\mathcal{I}_c(i, j))) \quad (9)$$

This ensures noise for the negative values are the same as the positives with the corresponding magnitude. The images have negative values because of a bias pedestal applied to the level 0 data set at approximately 100 DN.

3.2. Pre-processing

After a noisy images is created, using the aiapy package, both $\mathcal{I}_c(i, j)$ and $\mathcal{A}_c(i, j)$ are transformed by way of registering the image (Cite aiapy here). This function scales the image to a plate scale of 0.6 arcsec per pixel and rotates the image so that the y-axis is aligned with solar North for each channel. A byproduct of this transformation is that the values are now continuous instead of discrete. The images are also normalized by exposure time. We call this transformed state level 1.5. The sunpy package is also used in conjunction with aiapy and was used for extracting regions of interest (ROI) from the images (SunPy Community et al. 2015).

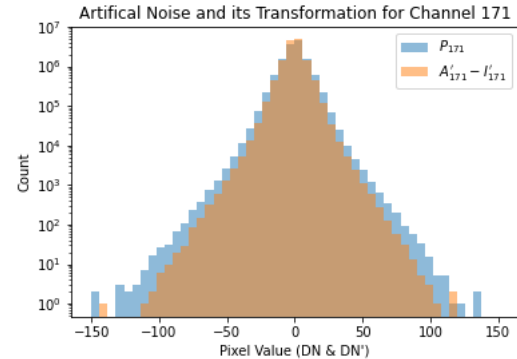


Figure 1. Log-y histogram of pixel noise values for a 3668x3668 ROI of an AIA 171Å image. This is plotted without exposure time normalization which is a linear transformation and would not change the shape of the distribution. It can be seen that the register function from aiapy slightly transforms the distribution.

Once we compute $\mathcal{I}'_c(i, j)$ and $\mathcal{A}'_c(i, j)$ the final pre-processing step is to scale the channels. This scaling is done so the model is not bias toward the high SNR channels. Let the training and test set of images be

denoted as

$$X'_c(i, j)\{\text{train} \parallel \text{test}\} = \{X'_c(i, j)(1), X'_c(i, j)(2), \dots\} \quad (10)$$

respectively. The channel-wise scaling is then done by dividing by the channel-wise median of the set-wise mean as shown by

$$X'_c(i, j)\{\text{train} \parallel \text{test}\}_{\text{scale}} = X'_c(i, j)\{\text{train} \parallel \text{test}\} / \text{median}_c(\text{mean}_{\text{set}}(X'_c(i, j)\{\text{train}\})) \quad (11)$$

3.3. Model

The proposed model is a stacked autoencoder with a skip connection as shown in Figure 2. By utilizing the skip connection the autoencoder only has to learn to remove the noise instead of additionally reconstructing the signal which significantly reduces the training time.

The model parameter decisions were done using a testing suite with different combinations and compared using test statistics. The model parameters chosen are Adam optimizer, L1 loss, LeakyReLU hidden activation, Linear output activation, and a hidden layer configuration of [6,4,6]. Many test statistics were used to compare, the most useful one being a Chi-squared between the histograms of the isolated added noise and removed noise. The histogram comparison is used so that high value pixels do not dominate and the sum is not extremely large as the sum would be over millions of pixels. A bin size of 100 is used with range of $\pm 3\sigma$. The statistic is defined as

$$\chi_c^2 = \sum \frac{(\text{hist}(\mathcal{A}'_c - \mathcal{I}'_c) - \text{hist}(\mathcal{P}'_c))^2}{\text{hist}(\mathcal{P}'_c)} \quad (12)$$

Using this the model parameters are chosen and the hyperparameters tuned to be a batch size of 250, epoch size of 15, and initial learning rate of 0.0001.

4. RESULTS & DISCUSSION

Four training image channel sets were selected for the training set, two from an active region (AR) and two from a quite sun (QS) region. The ROI of the image is 1000x1000 arcsec which gives 1668x1668 pixels, per the standardized plate scale. A ROI is used instead of the entire solar image so the solar limb and background space is not included. The training set is then approximately 11 million channel-wise pixel sets. One significant benefit of this channel-wise method instead of a convolutional method is the extremely low requirement for training data.

In the following figures, the images are plotted on the same scale as each other. This means the colormap

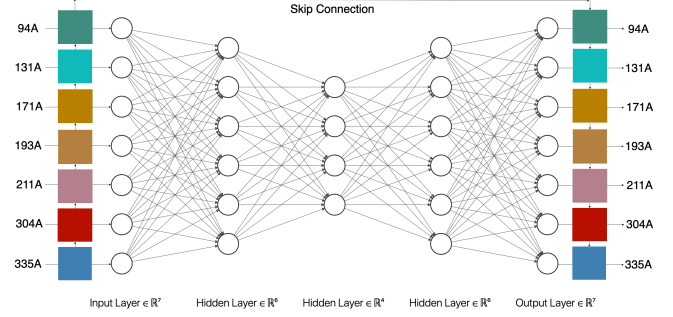


Figure 2. Diagram of the autoencoder architecture. The model is trained with $\mathcal{A}(i, j)$ channel-wise pixel data as the input and $\mathcal{I}(i, j)$ as the objective. The bottleneck ensures the data is represented with reduced dimensionality. This is intended to have the effect that signal is preserved and noise removed in the encoded state. With the addition of the skip connection, the model only has to learn the "anti-noise", which is the correction added to original image to remove the noise.

maximum and minimum are set to the maximum and minimum pixel values found across the original, noisy, and denoised images for each channel. If this is not done, if a pixel that goes through the model is an extreme outlier, the entire image would appear smoother as the rest of the image would be colored using a smaller section of the colormap. However, by coloring the images this way, if a denoised image is scaled such that its range is now smaller, it would also appear smoother. We do not believe this is happening. Looking at our chi-squared values in Table 1, it indicated that denoising is actually happening and the smoothing effect is not a misattribution to image values over a smaller range,

Table 1. Chi Squared statistic, shown in Equation 12, for the defined model architecture and parameters. The values represent the difference between the artificially added noise and removed noise. The white box in Figure 3 is the region used to calculate these values. The low SNR channels have low chi-squared statistics indicating the model correctly learned to remove this noise. The high SNR channels do not, the reason is not yet understood. Much work was put into changing the architecture of the model to potentially fix this, such as only using the loss from one of the high SNR channels, but no configuration worked well.

Channel	χ_c^2
94Å	1.84
131Å	1.05
171Å	96.44
193Å	148.31
211Å	32.13
304Å	70.51
335Å	1.51

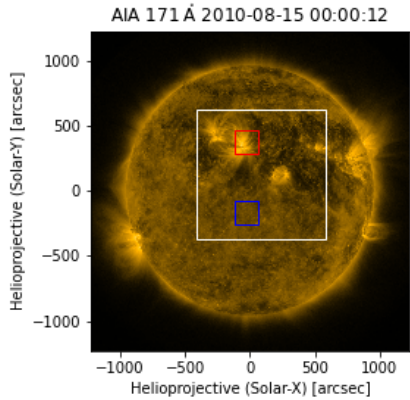


Figure 3. Solar image showing the subsection used for the artificially noisy test data. The white box is the entire denoised section, the red box is the AR region, and the blue box is the QS region. These regions align with the images in Figure 6.

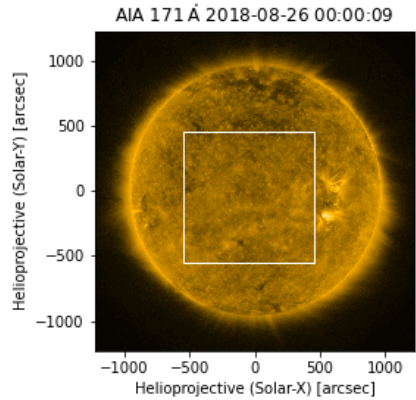


Figure 5. Solar image showing the subsection for the QS images in Figure 8. A large QS region was needed to see the waffle patterns in the removed noise.

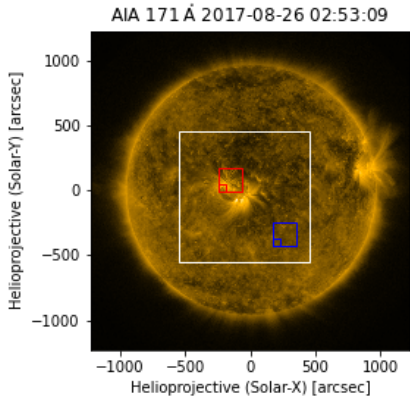


Figure 4. Solar image showing the subsection used for the unmodified test data from later in the mission. The white box is the entire denoised section, the red box is the AR region, and the blue box is the QS region. The white region aligns with the AR images in Figure 7. The large blue and red sections align with the images in Figure 9. The smaller colored sections represent the very zoomed images found in Figure 10.

The authors acknowledge support from NASA's SDO/AIA contract (NNG04EA00C) to LMSAL. AIA is an instrument on board the Solar Dynamics Observatory, a mission for NASA's Living With a Star program.

DENOISE

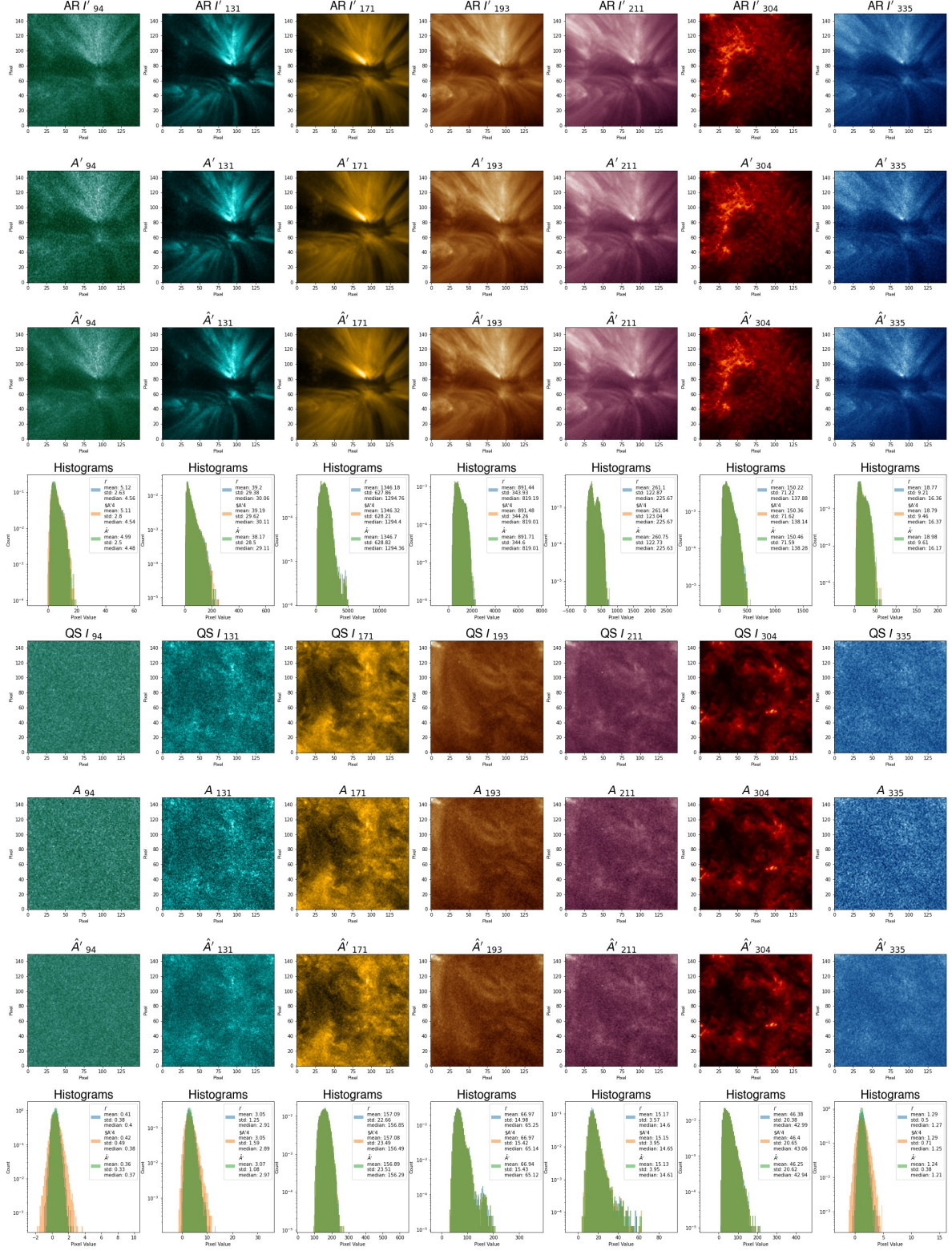


Figure 6. The original, artificially noisy, and denoised images from 2010 data. At this scale, one can visually see the effects of the denoising model on the low SNR channels for both the AR and QS regions. In addition, the histograms indicate denoising as well. For example, in the AR 94 \AA set of images, the standard deviation goes from 2.63 to 2.8 to 2.5 respectively. One would expect the noisy image to have a higher standard deviation, which it does in all cases, and the denoised image to reduce the standard deviation by removing the noise. This happens for all the low SNR channels. One would also expect the mean to be constant throughout which is the case for the addition of noise. However, as an unwanted effect, the mean and median are slightly shifted in the denoised image.

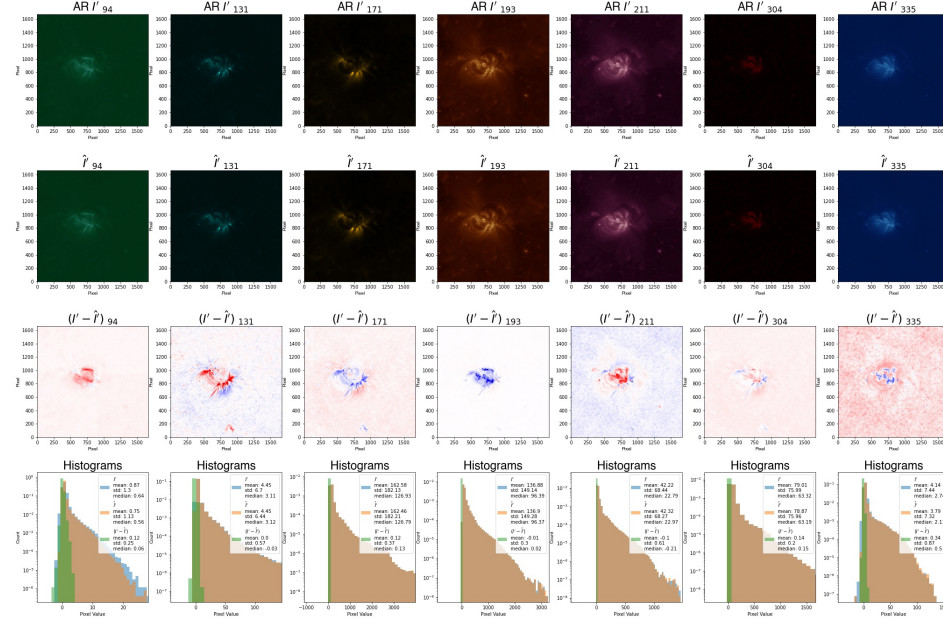
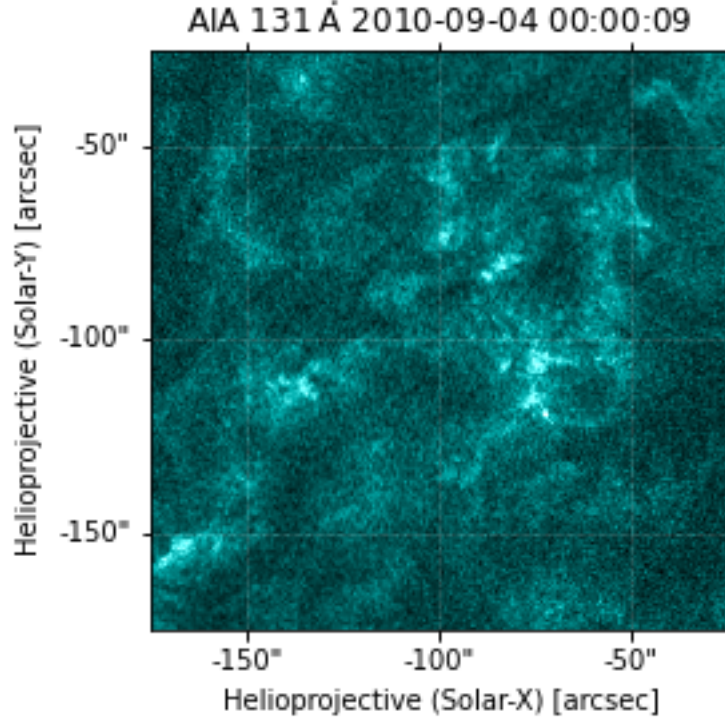


Figure 7. Denoised images from Figure 5. At this scale, not many differences can be seen between the two images. The removed noise plot represents the difference between the original and denoised image where the colormap is centered at 0. It can be seen in the comparison of the removed noise for the AR 131Å & 171Å cases that there is significant cross-correlation between the two. It is believed that the low SNR channels denoise well because they use the strong signal from the high SNR channels to return to their expectation value. As a result of this, some "cross-talk" is expected. This also explains why the high SNR channels themselves do not denoise, as there are no better channels to take the signal from. Looking at the histograms, it can be seen the standard deviation of the removed noise is consistent across channels but obviously has little effect on channels where the mean is much larger. Additionally, some "cross-talk" is not only allowable, but physically correct. The ground truth signal is correlated across channels despite being imaged at different wavelengths.



:0-2:0 i+-i

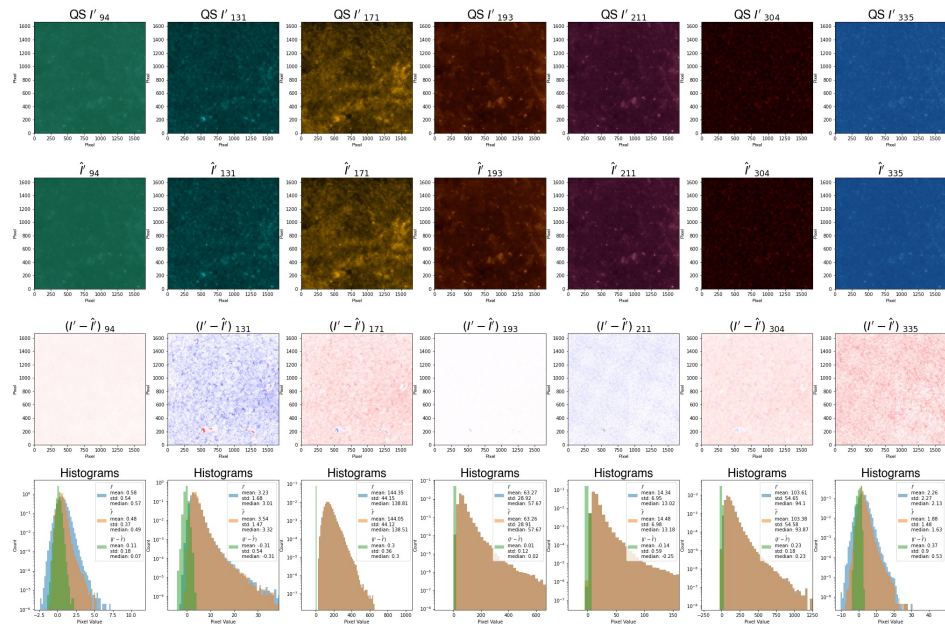


Figure 8. Denoised images from Figure 5. In the QS 335Å removed noise image, one can see a waffle pattern. This pattern is a result of the rotation interpolation done by the aiapy method and is present in low SNR channels. In addition to denoising, it appears this model also helps remove/reduce this waffle pattern.

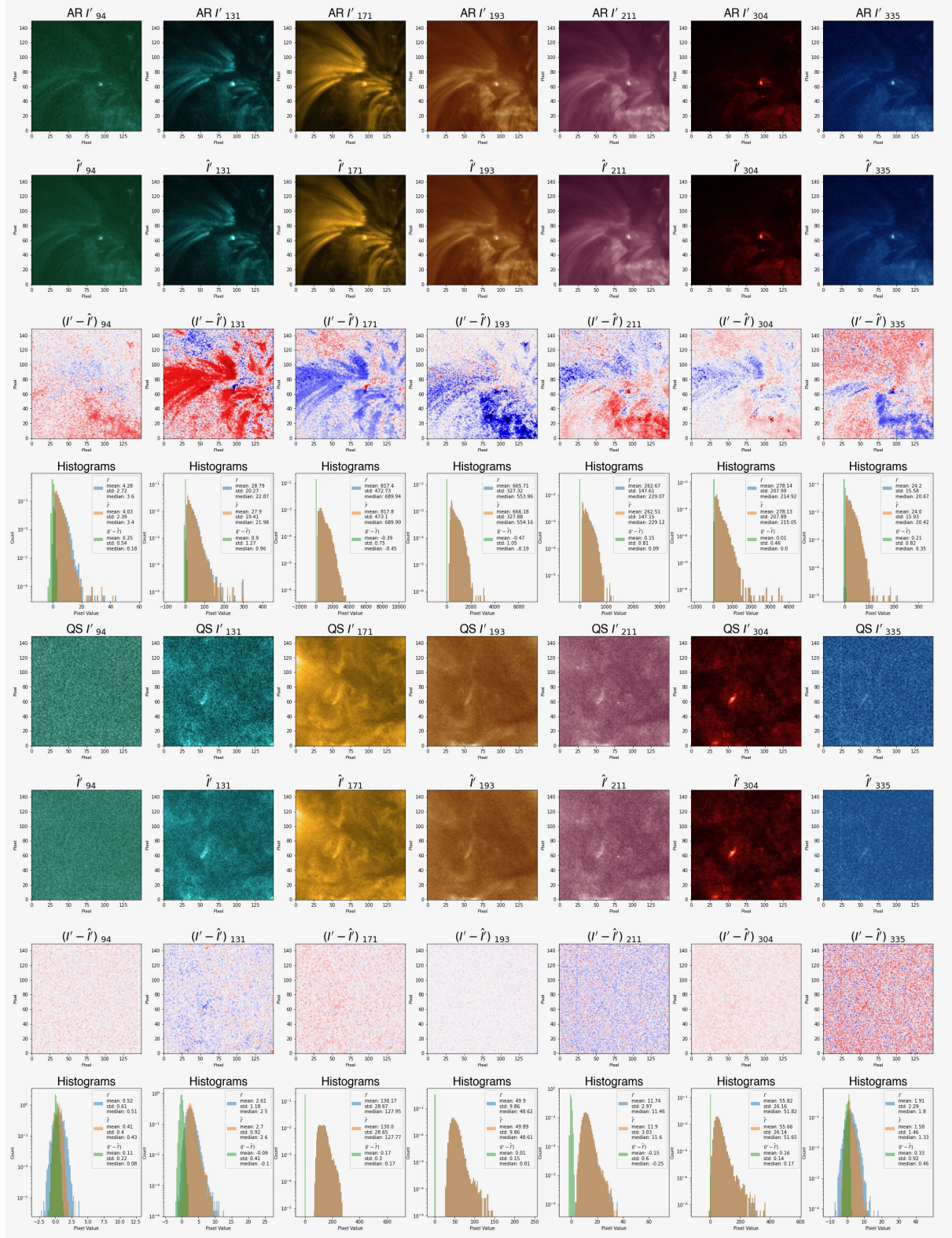


Figure 9. Denoised images from Figure 5. The low SNR channels (94\AA , 131\AA , 335\AA) exhibit significant improvement in their noise reduction. The high SNR channels struggle to remove noise. Ideally, all channels would show improvement, however the high SNR channels are already decent given their nature so improving the low SNR channels is a much needed improvement. Additionally, looking at the AR images, there appears to be very little denoising even in the low SNR channels. Just as the high SNR channels are difficult to denoise, the high signal active regions of the low SNR channels are equally hard to denoise.

DENOISE

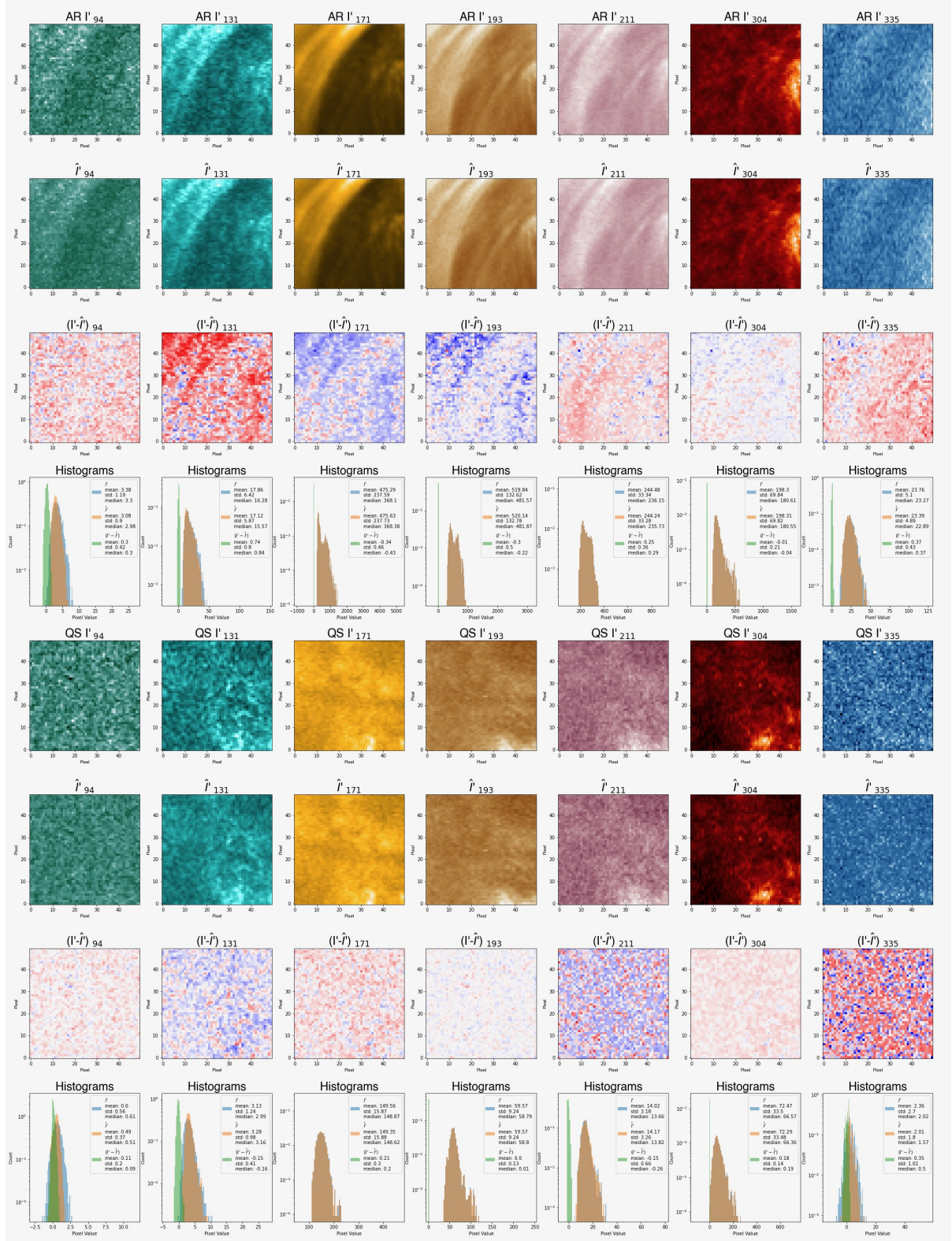


Figure 10. Denoised images from Figure 5. In these very zoomed in images, one can see the exact effect on a pixel-wise basis much clearer. Ideally, whether the removed noise is positive or negative would be spatially uncorrelated. However, due to the 'cross-talk' there appears to be some groupings which are corrected to the groupings in the higher SNR channels.

REFERENCES

- Boerner, P. F., Testa, P., Warren, H., Weber, M. A., & Schrijver, C. J. 2014, *SoPh*, 289, 2377,
doi: [10.1007/s11207-013-0452-z](https://doi.org/10.1007/s11207-013-0452-z)
- DeForest, C. E. 2017, *ApJ*, 838, 155,
doi: [10.3847/1538-4357/aa67f1](https://doi.org/10.3847/1538-4357/aa67f1)
- Hurlburt, N., Cheung, M., Schrijver, C., et al. 2012, *SoPh*, 275, 67, doi: [10.1007/s11207-010-9624-2](https://doi.org/10.1007/s11207-010-9624-2)
- Lemen, J. R., Title, A. M., Akin, D. J., et al. 2012, *The Atmospheric Imaging Assembly (AIA) on the Solar Dynamics Observatory (SDO)*, ed. P. Chamberlin, W. D. Pesnell, & B. Thompson (New York, NY: Springer US), 17–40, doi: [10.1007/978-1-4614-3673-7_3](https://doi.org/10.1007/978-1-4614-3673-7_3)
- SunPy Community, T., Mumford, S. J., Christe, S., et al. 2015, *Computational Science and Discovery*, 8, 014009,
doi: [10.1088/1749-4699/8/1/014009](https://doi.org/10.1088/1749-4699/8/1/014009)